Industry Canada CRC

A COMPARISON OF MODELLED AND MEASURED HF ANTENNA ARRAY PATTERNS

by

R.W. Jenkins and L.E. Petrie

CRC TECHNICAL NOTE 96-002

September 1996
Ottawa

Industry and Science Canada Industrie and Science Canada

The work described in this document was sponsored by the Department of National Defence under Tasks 998426159 and 998445419.

Canada

A comparison of modelled and measured HF antenna array patterns

by

R.W. Jenkins
Comminucations Research Centre

and

L.E. Petrie
Petrie Telecommunications Ltd.

The work described in this document was sponsored by the Department of National Defence under Tasks 998426159 and 998445419

COMMUNICATION RESEARCH CENTRE INDUSTRY AND SCIENCE
CRC TECHNICAL NOTE 96-002

Canada

September 1996
Ottawa

ABSTRACT

The relative-phase response and gain patterns found by numerical modelling of an HF antenna array of vertical whip antennas were compared with the patterns found by actual measurements. While some features of the measured patterns agree with the model, other significant features did not. The disagreement could be due to ground inhomogeneities and other local features as well as differences between the actual and modelled antenna array such as discrepancies in antenna position and orientation, poor connections to ground radials, and differences in the modelled and actual antenna loading. In most cases where the elements were closely spaced, numerical modelling provided a somewhat better estimate of the antenna gain and relative-phase response patterns than the simple assumption of azimuth-independent gains and a relative phase response consistent with a spherical wavefront centered on the transmitter. However, for more remote antenna elements, modelling did not provide a better estimate; nor did it provide a better estimate for the lowest modelled frequency. Actual pattern measurements, on the other hand provided significantly better pattern estimates in all cases.

RÉSUMÉ

La réponse en phase relative et les patrons de gain obtenus par modélisation numérique d'un réseau d'antennes HF à éléments verticaux sont comparés aux patrons obtenus par des mesures. Malgré le fait que certaines caractéristiques des patrons mesurés apparaissent aussi dans la modélisation, certaines caractéristiques importantes ne sont pas expliquées par le modèle. Ceci peut être dû à des inhomogénéités du sol et d'autres caractéristiques locales, ainsi qu'à des différences entre le réseau d'antennes lui-même et son modèle, comme des divergences dans la position et l'orientation des antennes, de mauvaises connexions au réseau de terre et des différences de charge d'antenne entre le modèle et le système mesuré. Dans certains cas, lorsque les antennes étaient très rapprochées, la modèlisation numérique fournissait un meilleur estimé de la réponse en phase relative et des patrons de gain d'antenne que la supposition simplificatrice du gain indépendent de l'azimuth, et la réponse en phase relative consistante avec un front d'onde sphérique centré au transmetteur. Cependant, pour des éléments d'antenne plus éloignés, et même pour des éléments rapprochés en utilisant la plus basse fréquence disponible, la modélisation n'a pas fourni de meilleur estimé. D'un autre côté, les mesures de patrons d'antennes ont fourni de bien meilleurs estimés dans tous les cas.

EXECUTIVE SUMMARY

Knowledge of the element gain and relative phase patterns in an antenna array is necessary in many HF radio systems (e.g., radar, direction-finding). The present technical note compares the antenna patterns found using numerical modelling with those measured, for an HF antenna array consisting of a number of vertical whip antennas interspersed with other (unused) elements. A recently refurbished airborne antenna pattern measurement system using differential GPS positioning was used to obtain the element patterns; the modelling was performed using NEC2 software. Separate ground conductivity measurements provided appropriate ground parameters for the model.

The measured and modelled patterns were found to agree in some, but not all, of their features. Substantial differences were noted which could be attributed to ground inhomogeneities, a layered ground, misalignments in antenna positioning and orientation, possible poor ground-radial connections, as well as other unaccounted-for local features.

In the absence of any pattern information, the simplest assumptions that could be made for an array of vertical whip antennas is that the antenna gains are azimuth-independent, and that the relative phase response of different elements is that predicted on the basis of a spherical wavefront centered at the transmitter (i.e., plane wave for distant transmitters). Typical errors in the gain patterns resulting from use of the azimuth-independence assumption were found to lie between 0.47 to 1.63 dB rms, with the largest errors occurring at low elevations, where ground conductivity played a large role in the gain, and for antennas close to other conducting elements which distort the patterns away from azimuth independence. The corresponding errors in relative phase response with the spherical wavefront assumption varied from 4.2° to 14.6° rms, depending on the antenna and radio frequency.

Use of the numerical model instead of the assumptions reduced the errors in some but not all cases. The rms errors (in gain and relative phase response) were reduced at the higher HF frequencies of 11.5 and 18.0 MHz, for the antennas close to other conducting elements. However the gain errors remained the same or became slightly worse, when the model was applied at 5.1 MHz or to an antenna remote from other radiating elements. The relative phase errors were substantially worse with numerical modelling at 5.1 MHz for closely spaced elements. For the remote element modelled at 5.1 MHz, as well as for all antennas at higher frequencies, the relative phase errors were less with modelling.

A marked reduction in the rms errors in gain and relative phase response was noted when the pattern measurement system was used to obtain these quantities.

On the basis of these findings, it is recommended that actual pattern measurement be used in HF systems where precise knowledge of the antenna patterns is required. Pattern measurements are required to be made at many closely-spaced frequencies spanning the frequency range of operation, in order to allow accurate interpolation to intermediate frequencies. As ground conditions can change significantly with season, (e.g. frozen vs. thawed ground) it may also be neces-

sary to measure the patterns at different representative times of year. A large number of measurements can be costly. If measurements are not feasible, then modelling can be useful in obtaining patterns for cases where the antenna elements are closely spaced. Modelling may also be of aid in the frequency-interpolation of measured patterns. When modelling is used, it is very important to know and model precisely the locations and orientations of the conducting elements, as well as the ground parameters, and to locate the array in a level area over which the ground parameters are constant.

1.0 Introduction

Knowledge of the antenna array element patterns is important to HF radio systems: radar, direction-finding, and communications. The information required for many array applications includes both the amplitude and phase responses of the elements over all directions and frequencies of interest. This information is difficult to obtain: comprehensive direct measurements using airborne transmitters can be time-consuming and costly, and numerical modelling techniques suffer from the limitations imposed by incomplete knowledge of the local antenna environment, as well as by limitations in the modelling software.

Recently a relatively inexpensive pattern measurement system developed at the CRC was refurbished, to allow both amplitude and relative-phase response measurements to be made. This system was used to obtain antenna patterns for an HF array of vertical whip antennas in the Ottawa area. The system and the results of the measurements are presented in a recent CRC report [1]. They show significant azimuthal variations in the patterns of the elements, as well as significant variations in the relative phase responses, away from those expected on the assumption of a spherical wavefront centered on the transmitter. By comparing the patterns of different elements in the array for which the interelement geometry was similar, it was deduced that some of the pattern variations could be explained by the antenna element interaction, but that a significant remainder could not. This remainder was attributed to localized ground effects and unconsidered differences in the elements and their ground radials.

In order to further explore the sources of the pattern variations, and also to determine the degree to which the HF antenna patterns (gain and phase) could be predicted, numerical antenna pattern modelling was undertaken. This modelling was performed using NEC-2 modelling software, on the same antenna array used for measurements, and took into account all conducting elements in the array and its vicinity (vertical whips, ground radials), the actual antenna matching, and a constant ground conductivity. The modelling was performed for frequencies and directions similar to those used in the measurements.

The present technical note compares the modelled antenna patterns with those measured, and discusses the relative errors and benefits resulting from use of these approaches to obtaining antenna array patterns.

2.0 Measurements

The Xeledop antenna pattern measurement system and the measurements are described in the previous report [1]. Those items pertinent to the present document are described herein.

The pattern measurement system consisted of a small transmitting unit including a dipole antenna, which was towed behind a light aircraft. The transmitter emitted one of several tones in the HF range. The location of the transmitter had to be known accurately in order that relative-phase as well as gain response measurements could be made. This was facilitated through the use of differential GPS (global positioning system) technology. A GPS receiver was mounted in the aircraft, where it received UHF communication from a second (reference) GPS receiver on the ground, as well as from the GPS satellites.

The pattern measurements were executed by flying the aircraft in circles around the array, at various heights and distances, to obtain the azimuthal patterns for various elevation angles. In addition, several 'radial' runs were made, in which the aircraft flew in straight lines over the array. The radial flights were used to obtain elevation patterns for several azimuths. The signal strength received by the antenna elements was measured and recorded with a sampled-aperture digital recording system provided by the DND owner of the antenna array. Azimuthal antenna patterns were measured at elevation angles of approximately 4.5°, 11°, 19°, 31°, and 49°, and at frequencies of 5.1, 9.3, 11.5, 15.1, and 18.0 MHz.

3.0 Antenna Array

The antenna array consisted of eight elements selected from the twenty-four inner-circle elements of a Pusher array normally used for direction finding, plus four additional vertical whip antennas. Figure 1 (reproduced from [1]) shows a plan view of the array. Array parameters used in the numerical modelling are listed in Table 1.

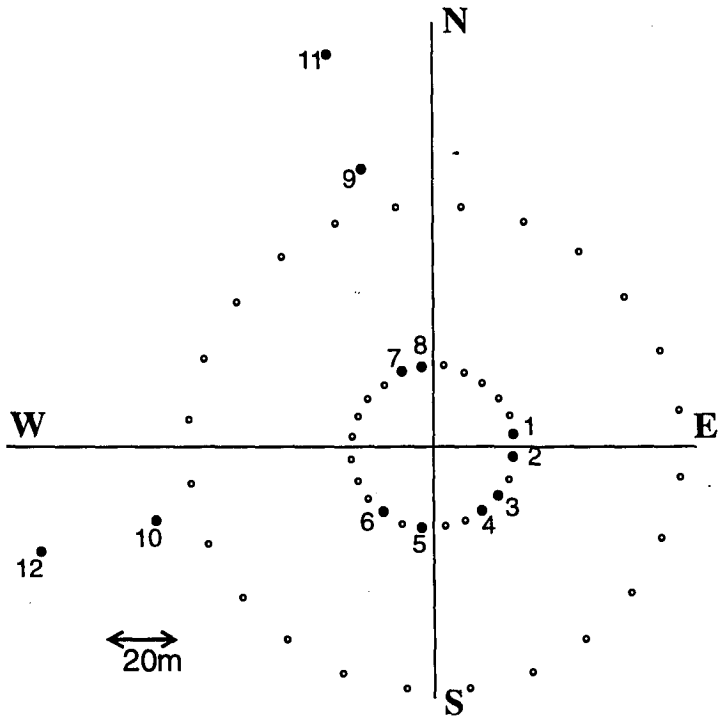

Figure 1. Plan view of antenna array, showing selected elements

Table 1: Antenna Array Parameters

Inner-circle elements:	25-m radius, 24 antennas separated 15° in azimuth, in directions 7.5°, 22.5°, . . . 352.5° E of N. 2-in diameter aluminum, height 20 ft, antenna feed 7 ft above ground 8 ground radials per element, 8 ft length, separated 45° in azimuth, with one radial aligned toward array center.
Outer-circle elements:	75-m. radius, 24 antennas separated 15° in azimuth, in directions 7.5°, 22.5°, . . . 352.5° E of N. 2-in diameter aluminum, height 40 ft, antenna feed 13 ft above ground 8 ground radials per element, 24.3-ft length, separated 45° in azimuth, with one radial aligned toward array centre.
Additional elements:	4 elements, in directions 255° and 345° E of N, at 88- and 125-m radii 2-in diameter aluminum, height 20 ft, antenna feed 7 ft above ground no ground radials, 12-in square ground plate, 0.024 in thick.

4.0 Modelling Technique

The amplitude and phase of the signal received at a number of selected antennas was computed using a NEC2 computer program. The program was expanded to accommodate 1500 segments for these computations. Alterations were made to the program in order to extract phase information on the signal.

In modelling the individual vertical whip elements, the element support structure (consisting of three nylon ropes separated by 120° in azimuth and connected to individual anchors) was ignored. The base grounding plates for both the inner- and outer-circle elements were represented by eight radial wires uniformly spread over 360° in azimuth and connected to the base of the vertical whip. The ground wires, which were covered by an insulating jacket, were assumed to be 0.2 inches above ground. The 12-inch square ground plates of the four additional antenna elements were represented by eight 7-inch long radials of #12 wire equally spaced over 360° azimuth.

As the modelling required a significant amount of computation and therefore time, it was considered highly desirable to find ways to reduce the effort. An initial set of calculations for the inner-circle antennas showed that their patterns, both amplitude and phase, were identical, when the patterns were rotated according to the antenna position in the circle. (This result indicates that the modelled interaction between inner-circle antennas and the four additional antennas, which

did not have the same symmetry as the inner-circle elements, was negligible.) It was therefore not necessary to present the results for all inner-circle elements separately; instead, a single representative element could be used.

Initially it was thought that the modelling would have to assume the same transmitter location as the Xeledop for a proper comparison. However, in the initial modelling, it was found that the model patterns, both gain and relative-phase, that were found using the actual Xeledop locations, agreed with those based on far-field computations (within 0.2 dB and 1° respectively). On this basis, since this represented a considerable computational saving, far-field calculations were used for the modelling.

Reference [2] provides further details of the modelling. In this reference, a relatively poor ground (conductivity $\sigma = 0.001$ mhos/m, dielectric constant $\varepsilon = 4$), was used to compute the patterns, as the nature of the ground appeared to support this assumption. However, an initial comparison of measured and modelled patterns suggested that the ground was more highly conducting than previously thought. A set of surface-wave signal strength measurements, conducted to check this finding, showed the ground conductivity to be approximately 0.02 mhos/m. The model was rerun using the revised ground conductivity; the results are reported in the present paper.

Modelled patterns were calculated for three frequencies: 5.1, 11.5, and 18.0 MHz. Azimuthal patterns were found by incrementing the azimuth in 1° steps over a full 360°, at fixed elevation angles of 4.5°, 11°, and 19°. The elevation patterns were found for azimuths of 9°/189° and 91°/271° E of N. (The previously measured patterns [1] were conducted for these frequencies, elevations and azimuths. The elevation patterns corresponded to straight-line paths over the array, having one azimuth on approach, and another azimuth 180° away on departure.)

5.0 Results

5.1 Initial Results Using Poorly Conducting Ground

Figure 2 shows the azimuthal gain patterns for antenna #5 an inner-circle element (see Figure 1), found from measurements and from modelling under the assumption of a poorly conducting ground ($\sigma = 0.001$ mhos/m, $\varepsilon = 4$). Patterns are shown for the three operating frequencies modelled, 5.1, 11.5, and 18.0 MHz, and for an elevation angle of 11°.

The model azimuthal variations in gain shown in Figure 2 differ somewhat from those measured, although there are some similarities. The more rapid gain variations with azimuth found using the model at the two higher frequencies agree somewhat in their azimuthal dependence with those measured, but are noticeably smaller in amplitude.

The difference from spherical phase-front values in the relative phase between antennas #5 and #1 is plotted as a function of azimuth, in Figure 3. Plots are included for the three modelled frequencies. The elevation angle of the plots is 11°, as before.

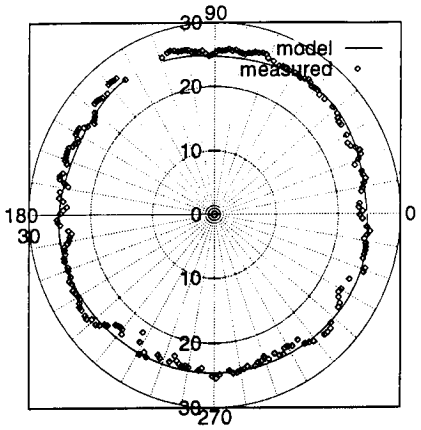

5.1 MHz

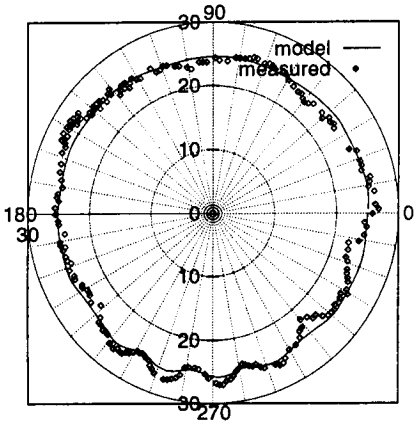

11.5 MHz

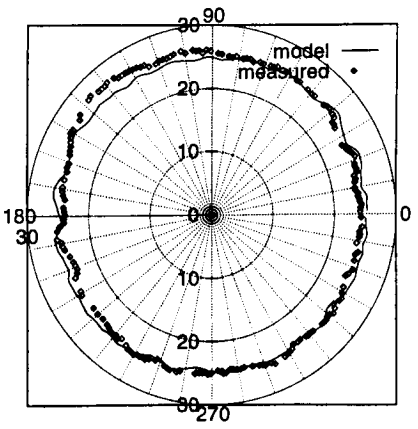

18.0 MHz

Figure 2. Measured and modelled azimuthal gain patterns for antenna #5, at an elevation angle of 11degrees, assuming a poor conducting ground (σ = 0.001 mhos/m, ε = 4) for the model.

Like the gain patterns, the relative-phase difference patterns do show some similarity between measured and modelled values, but there are significant differences as well. At 18.0 MHz, and to a lesser degree at 11.5 MHz, the phase variations found in modelling agree in their azimuthal dependence, but are much smaller in amplitude.

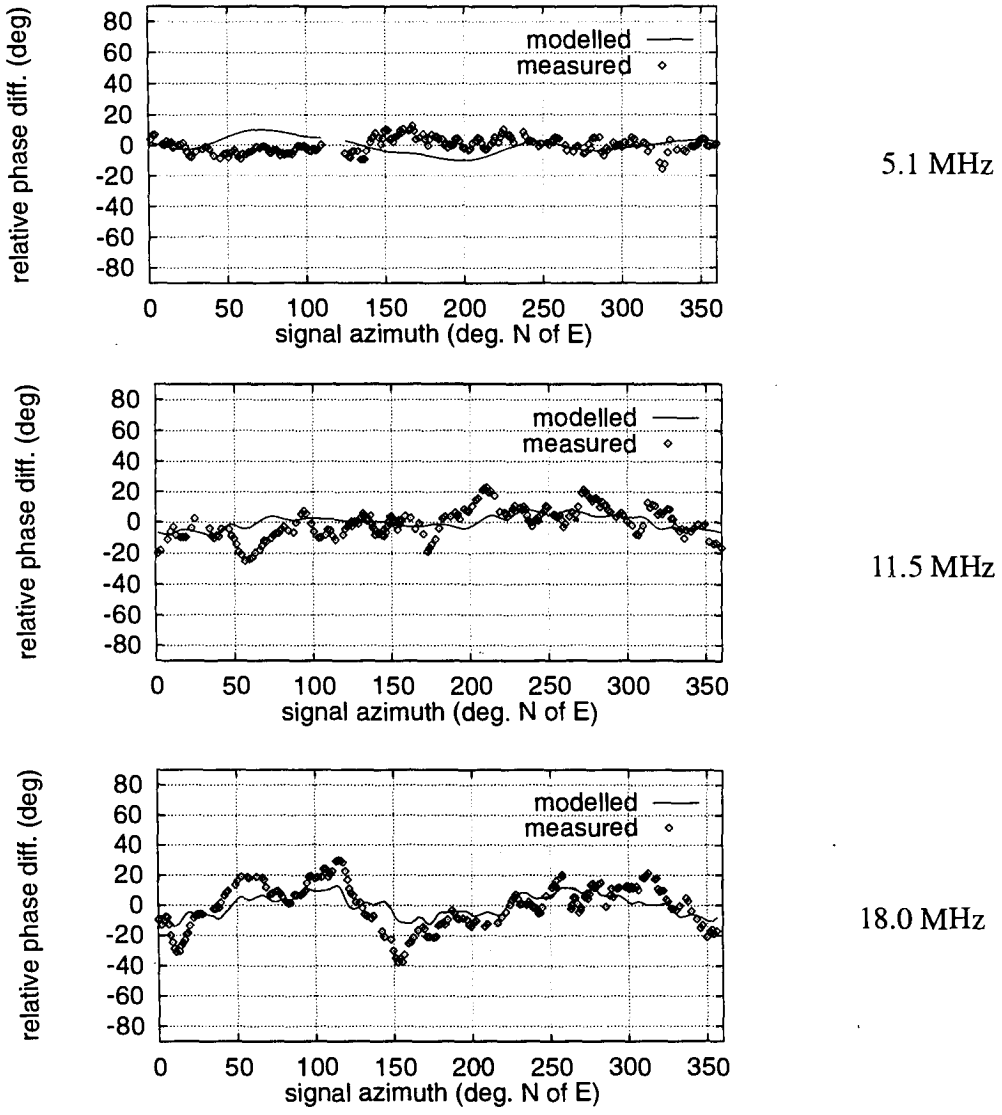

Figure 3. Measured and modelled azimuthal patterns of the difference from the spherical wavefront value in the phase response relative to antenna #1, for antenna #5 at an elevation angle of 11 degrees, assuming a poor conducting ground (σ = 0.001 mhos/m, ε = 4) for the model.

It was found that increasing the ground conductivity in the model increased the amplitude of the variations in gain and relative phase difference with azimuth. The small variations noted in Figures 2 and 3 for the model suggest that the chosen ground conductivity may have been too low.

Figure 4 shows both modelled and measured elevation gain patterns found for antenna #11, for the three frequencies 5.1, 11.5, and 18.0 MHz. In order to facilitate a comparison, the measured and modelled patterns shown are normalized to the same average value (25 dB) in the region of the nose (15 - 25°) of the elevation pattern.

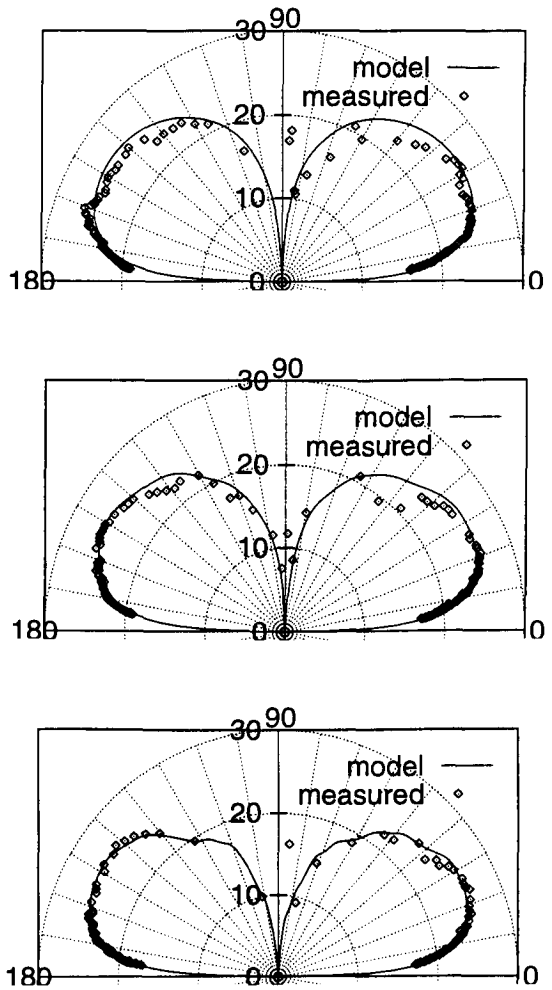

Figure 4. Measured and modelled elevation gain patterns for antenna #11, assuming a poor conducting ground (σ = 0.001 mhos/m, ε = 4) for the model, for an azimuth of 9/189 deg. E of N.

From Figure 4, the measured and modelled elevation patterns can be seen to be in approximate but not perfect agreement. The high-elevation gains found from the modelling tend to be larger than those observed, especially at the lower frequencies. In addition, a close examination of the lowest elevations shows the model predicts greater undercutting than is observed at the two higher frequencies. As the degree of undercutting is less for higher ground conductivities, this implies again that the ground conductivity used in the model was too low.

To resolve this question, surface-wave signal-strength measurements were used to obtain a value for the ground conductivity in the vicinity of the array. Measurements were made in several directions, up to distances of 2 km away, using an radio frequency of 9.2 MHz. The measurements gave a new value for the ground conductivity: 0.02 mhos/m.

5.2 Results Using Measured Ground Conductivity

Figures 5, 6, and 7 show the corresponding new azimuthal gain patterns, azimuthal relative-phase difference patterns, and elevation gain patterns found with the new ground conductivity.

Although considerable differences continue to exist between the modelled and measured azimuthal patterns, many of the observed features, both in gain and relative phase, appear to be well-explained by the model. The amplitudes of the model azimuthal variations in gain and relative phase are similar to those seen in the measurements. This is in contrast to the modelled variations for poor ground (Figures 2 and 3) which were substantially less than the measured variations.

Figure 5 shows azimuthal variations in gain of the order of 1 to 3 dB, depending on frequency. For some azimuths and frequencies, the model and measurements are in very good agreement (e.g., 11.5 MHz, variations in gain with azimuth between 210° and 300° N of E). For others there is significant disagreement: the measured patterns show variations which are not predicted by the model.

The azimuthal variations in relative phase response displayed in Figure 6 increase substantially with radio frequency. At the higher frequencies, the variations in relative phase found by the model generally agree with those measured; minor differences exist, notably in the more rapid variations. At the lowest (5.1 MHz) frequency, where the azimuthal variations in relative phase are small, there is little agreement between the model and the measured variations.

In Figure 7, the modelled and measured elevation patterns are seen to be in fairly good agreement. The agreement is better than with the previous (poor-conducting ground) model, especially at the higher angles. At low elevation angles, the elevation patterns for the 11.5- and 18.0-MHz frequencies show reasonable agreement. However, at 5.1 MHz, there is substantially more undercutting observed in the measurements than is predicted by the model. These results

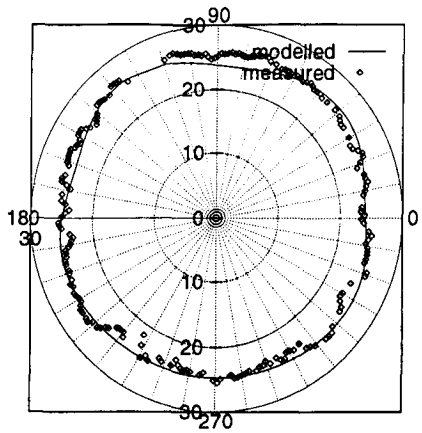

5.1 MHz

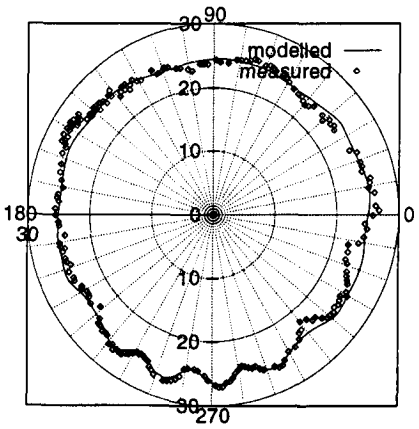

11.5 MHz

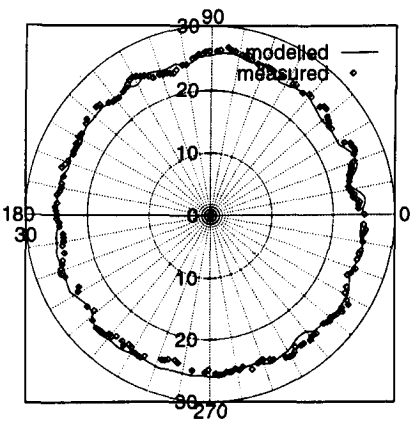

18.0 MHz

Figure 5. Measured and modelled azimuthal gain patterns for antenna #5, at an elevation angle of 11 degrees, using the measured ground conductivity (σ = 0.02 mhos/m, ε = 4) for the model.

suggest a layered ground in which the conductivity near the surface is substantially greater than at deeper depths. The greater skin depth at lower frequencies would cause the apparent conductivity to be lower and the undercutting of the elevation pattern to be correspondingly greater, at 5.1 MHz.

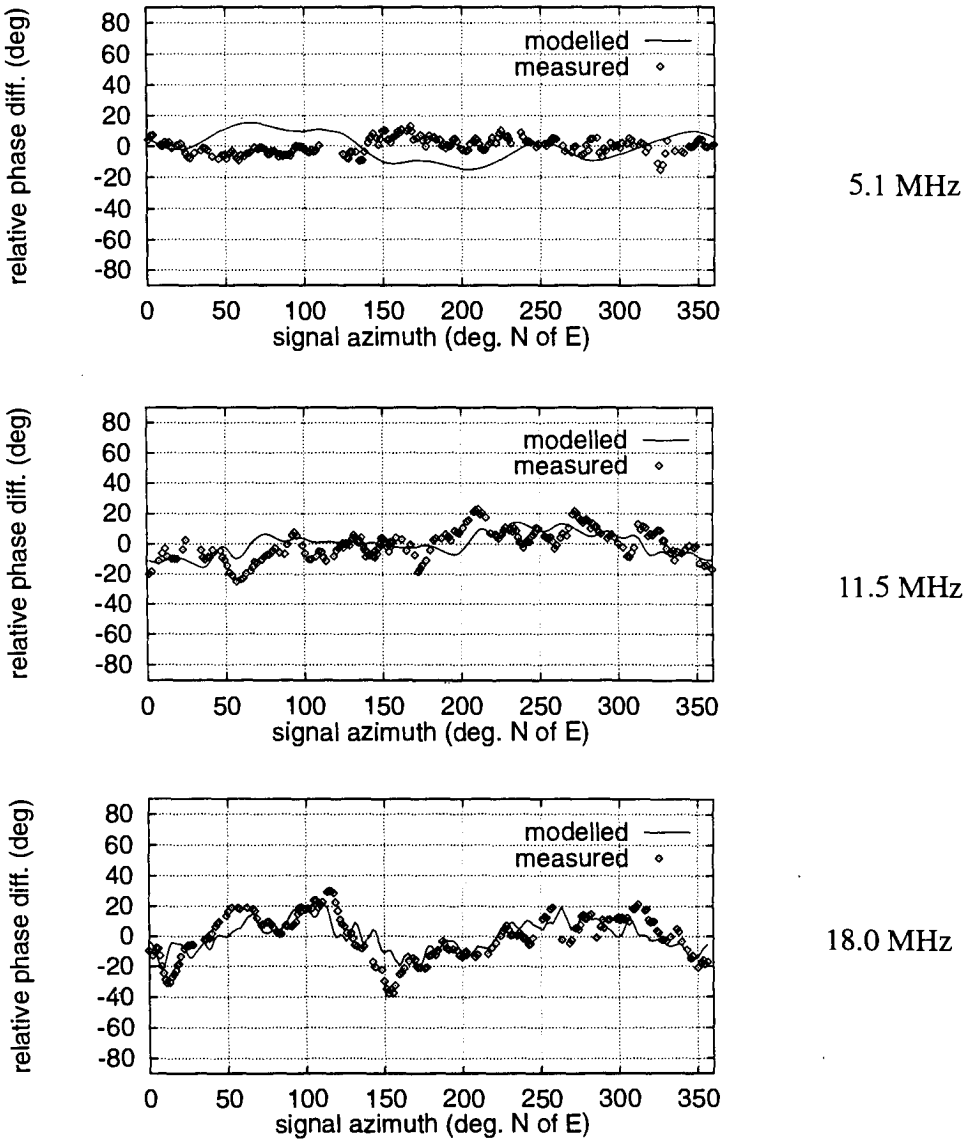

Figure 6. Measured and modelled azimuthal patterns of the difference from the spherical wavefront value in the phase response relative to antenna #1, for antenna #5 at an elevation angle of 11 degrees, using the measured ground conductivity (σ =0.02 mhos/m, ε = 4) in the model.

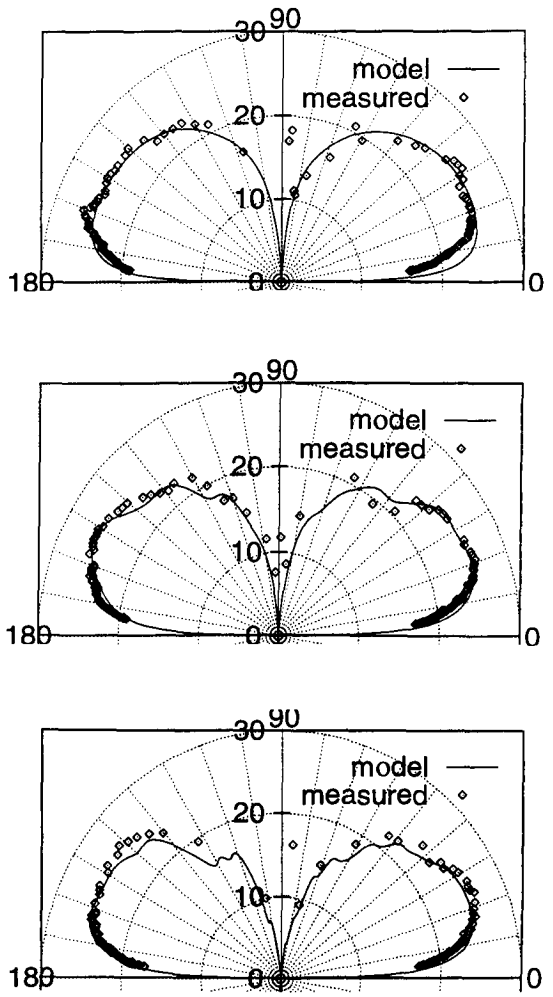

Figure 7. Measured and modelled elevation gain patterns for antenna #11 using the measured ground conductivity (σ = 0.02 mhos/m, ε = 4) for the model, for an azimuth of 9/189 deg. E of N.

5.3 Results for Various Element Antennas

The results presented so far are restricted to antenna #5, one of the element antennas in the inner circle of 24 antennas on a 25-m radius (Figure 1). The present section considers the results for antennas #9 and #11, which are quite different with regard to the conducting structures in their vicinities.

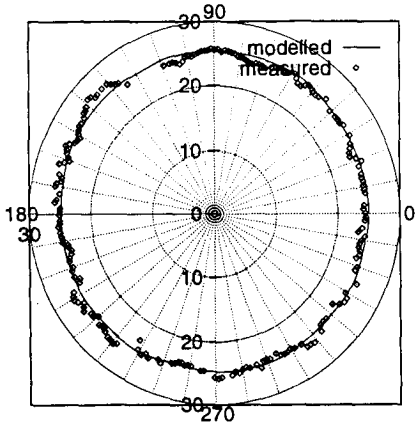

5.1 MHz

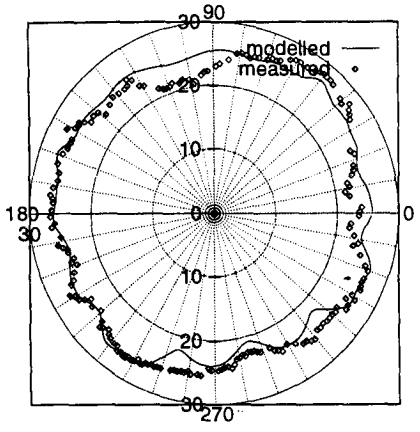

11.5 MHz

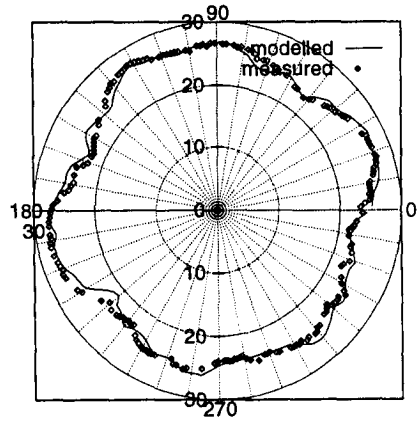

18.0 MHz

Figure 8. Measured and modelled azimuthal gain patterns for antenna #9, at an elevation angle of 11 degrees, using the measured ground conductivity (σ = 0.02 mhos/m, ε = 4) for the model.

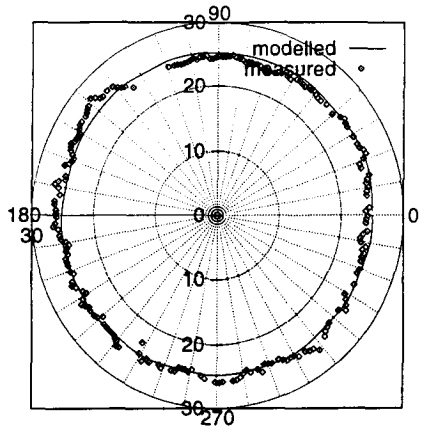

5.1 MHz

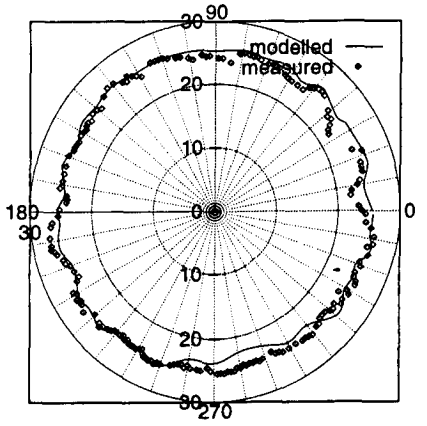

11.5 MHz

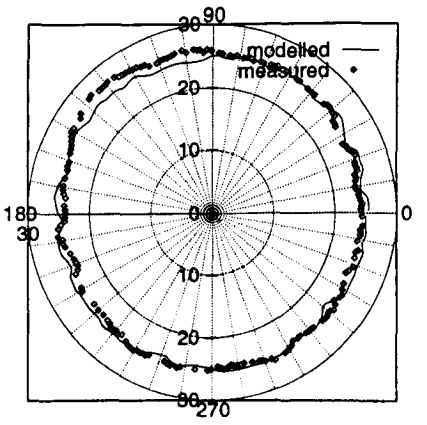

18.0 MHz

Figure 9. Measured and modelled azimuthal gain patterns for antenna #11, at an elevation angle of 11 degrees, using the measured ground conductivity (σ = 0.02 mhos/m, ε = 4) for the model.

Figures 8 and 9 show the measured and modelled azimuthal gain patterns for antennas #9 and #11, respectively, for the three frequencies 5.1, 11.5 and 18.0 MHz, at an elevation angle of 11°.

The most distorted patterns occur for antenna #9, at 11.5 and 18.0 MHz. This antenna is close to one of the large (40-ft whip) element antennas of the outer ring of the Pusher array with which substantial interaction can be expected. The large distortions in the measured azimuthal gain patterns are matched, at least in part, in the modelled patterns. However, the modelling predicts some rapid azimuthal variations which are not seen in the measurements (e.g., Figure 8, 11.5 MHz). This discrepancy might arise from differences in the ideal modelled conducting elements and the actual implementation (e.g., disconnected or misplaced ground radials, slight tilts away from vertical in the antenna orientations).

Antenna #11 is relatively distant from the other antennas in the array and can be expected to experience little interaction. Figure 9 shows its measured azimuthal variations in gain to be relatively small, with the possible exception of the 11.5 MHz frequency, where some rapid azimuthal variations are observed. For the most part, the modelling predicts somewhat smaller variations than are observed at 11.5 MHz.

The difference in relative phase from that of a spherical wavefront is plotted as a function of azimuth for antennas #9 and #11 with respect to antenna #1, in Figures 10 and 11, respectively. Measured and modelled patterns are shown for 5.1, 11.5 and 18.0 MHz at 11° elevation.

A comparison of Figures 6, 10, and 11 for antennas #5, #9, and #11 respectively reveals a pattern in the relative-phase difference patterns that is noted also for the gain patterns. The largest variations in relative-phase difference with azimuth occurs for antenna #9, which is expected to have a strong interaction with a nearby large outer-circle element. The smallest variations with azimuth occur for antenna #11, which is remote from all other elements and therefore is expected to interact only weakly. The azimuthal variations for antenna #5, which is one of a number of closely-spaced inner-circle elements, mostly lie between those of antennas #11 and #9.

As noted in the previous report [1] and in the previous section for antenna #5, the relative-phase differences depend strongly on frequency, being larger at the higher frequencies. At the 5.1-MHz frequency, relatively small variations with azimuth are noted, and there is little, if any, correspondence between the measured and modelled variations. At 11.5 MHz, much stronger azimuthal variations in relative-phase difference are noted, and there is substantial correspondence between the measured and modelled variations. At 18.0 MHz, the azimuthal variations are stronger yet, and the correspondence between measured and modelled values is perhaps greater. However. the differences in the measured and modelled values remain significant even at 18.0 MHz.

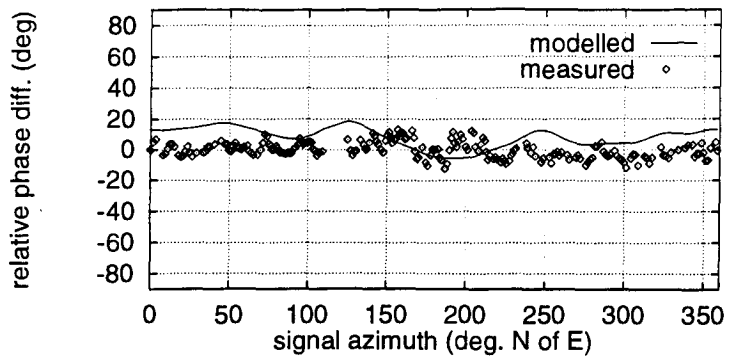

5.1 MHz

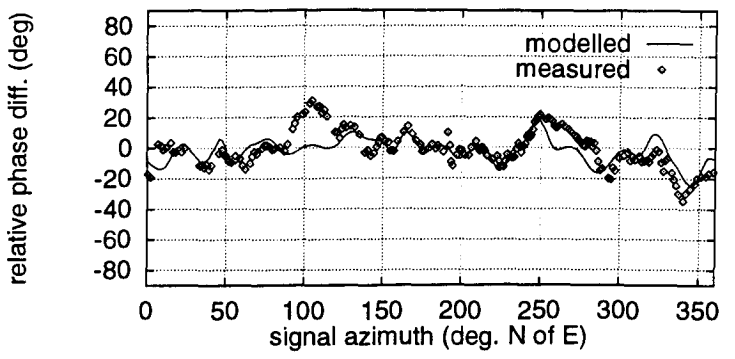

11.5 MHz

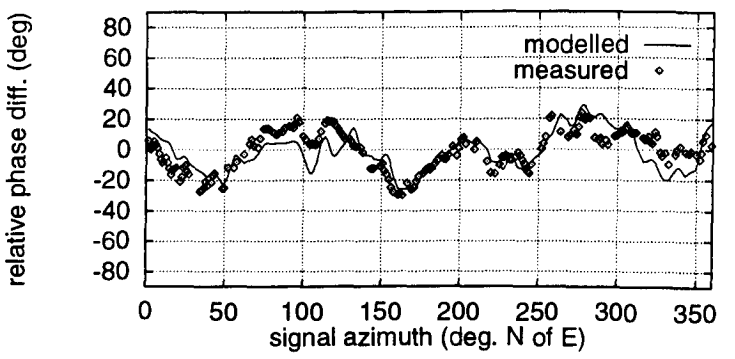

18.0 MHz

Figure 10. Measured and modelled azimuthal patterns of the difference from the spherical wavefront value in the phase response relative to antenna #1, for antenna #9 at an elevation angle of 11 degrees, using the measured ground conductivity (σ =0.02 mhos/m, ε = 4) in the model.

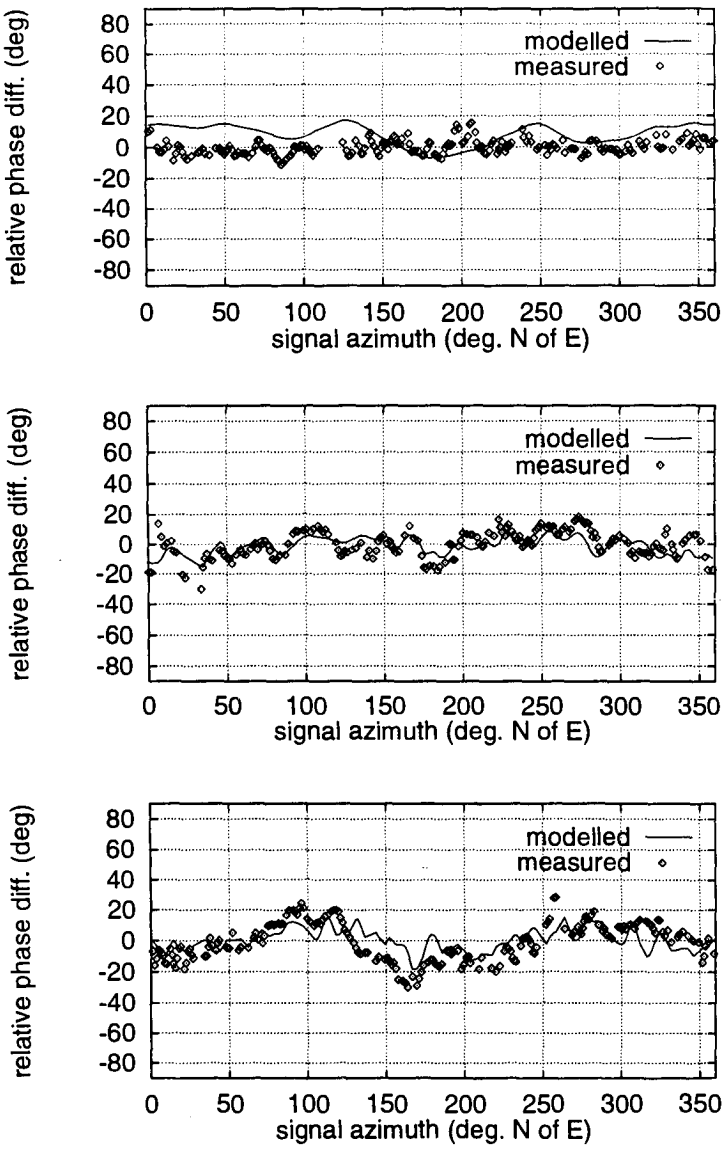

Figure 11. Measured and modelled azimuthal patterns of the difference from the spherical wavefront value in the phase response relative to antenna #1, for antenna #11 at an elevation angle of 11 degrees, using the measured ground conductivity (σ =0.02 mhos/m, ε = 4) in the model.

5.4 Implications for Pattern Errors

In the absence of any pattern information, a reasonable assumption is that the vertical-whip element antennas are azimuth-independent in their gain, and have a phase response corresponding to that of a spherical wavefront (plane wave for large distances). More accurate pattern information can be obtained from the modelling. The potentially most accurate information is that obtained by direct measurement, which in the absence of any measurement errors can be taken to be exact.

In order to quantify the uncertainty inherent in each of these approaches, the rms variation over azimuth was determined, both in gain and relative-phase difference from that expected from a spherical wavefront. The variation is expected to arise from two sources: the interaction between conducting elements in the presence of a constant ground; and harder-to-determine sources such as ground inhomogeneities, inaccurately placed elements, and the like. In addition, errors inherent in the measurement technique will affect the accuracy of measured patterns.

The measured rms variation over azimuth σ_{meas}, either in gain or relative phase, can be considered to be made up of the actual variation σ_{act}, and the rms variation arising from measurement errors ε_{meas}, according to

$$\sigma_{meas}^2 = \sigma_{act}^2 + \varepsilon_{meas}^2 , \qquad (1)$$

assuming that the measurement errors do not correlate with the actual variation.

Likewise, the observed rms difference over azimuth between the measured and modelled patterns can be considered to made up of the rms variation due to effects which are not taken into account in the modelling σ_{other}, and the rms variation due to measurement errors ε_{meas}:

$$\sigma_{obs}^2 = \sigma_{other}^2 + \varepsilon_{meas}^2 . \qquad (2)$$

The measurement error contributions σ_{meas} were found in the previous report [1], from a comparison of clockwise and counterclockwise circular flights.

The actual rms variation σ_{act} can be viewed as a measure of the error introduced by an azimuth-independent gain or spherical-wavefront phase response assumption (i.e., $\varepsilon_{iso} = \sigma_{act}$). Likewise the rms variation due to features ignored in the model, σ_{other}, is a measure of the error ε_{mod} introduced when the modelling is used to obtain the antenna patterns($\varepsilon_{mod} = \sigma_{other}$). ε_{meas} is a measure of the error introduced when the patterns are obtained by the measurement

technique.

Using equations 1 and 2, the potential rms 'errors' inherent in each of the three techniques were found, for the various azimuthal patterns. This was done for each of the three frequencies and elevation angles modelled. The results are provided in Tables 2 and 3 for gain and relative phase difference, respectively.

Table 2: Potential rms errors in antenna dB gain, arising from the three approaches to pattern estimation: azimuth-independent spherical phase-front assumption ε_{iso}, numerical modelling ε_{mod}, and actual measurement ε_{meas}.

ant. #5	5.1 MHz			11.5 MHz			18.0 MHz		
elevation	ε_{iso}	ε_{mod}	ε_{meas}	ε_{iso}	ε_{mod}	ε_{meas}	ε_{iso}	ε_{mod}	ε_{meas}
4.5°	1.17	1.23	0.23	1.41	1.01	0.70	0.74	0.73	0.37
11°	0.86	1.04	0.23	0.89	0.52	0.70	0.63	0.64	0.37
19°	0.67	1.19	0.23	1.05	0.74	0.70	0.70	0.75	0.37

ant. #9	5.1 MHz			11.5 MHz			18.0 MHz		
elevation	ε_{iso}	ε_{mod}	ε_{meas}	ε_{iso}	ε_{mod}	ε_{meas}	ε_{iso}	ε_{mod}	ε_{meas}
4.5°	1.37	1.49	0.24	1.63	1.35	0.69	1.48	0.80	0.32
11°	0.69	0.66	0.24	1.46	1.33	0.69	1.51	0.77	0.32
19°	0.47	0.45	0.24	1.51	1.15	0.69	1.26	0.78	0.32

ant. #11	5.1 MHz			11.5 MHz			18.0 MHz		
elevation	ε_{iso}	ε_{mod}	ε_{meas}	ε_{iso}	ε_{mod}	ε_{meas}	ε_{iso}	ε_{mod}	ε_{meas}
4.5°	1.56	1.68	0.27	0.75	0.95	0.72	0.45	0.72	0.35
11°	0.71	0.75	0.27	0.39	0.75	0.72	0.70	0.86	0.35
19°	0.47	0.54	0.27	0.60	0.57	0.72	0.99	1.08	0.35

Table 3: Potential rms errors in relative phase response difference, arising from the three approaches to pattern estimation: azimuth-independent spherical phase-front assumption ε_{iso} , numerical modelling ε_{mod}, and actual measurement ε_{meas} .

ant. #5 rel. to #1	5.1 MHz			11.5 MHz			18.0 MHz		
elevation	ε_{iso}	ε_{mod}	ε_{meas}	ε_{iso}	ε_{mod}	ε_{meas}	ε_{iso}	ε_{mod}	ε_{meas}
4.5°	4.2°	11.1°	1.2°	8.5°	8.6°	1.8°	14.1°	9.0°	2.2°
11°	4.9°	12.6°	1.2°	9.4°	8.5°	1.8°	14.6°	10.0°	2.2°
19°	4.4°	12.5°	1.2°	8.4°	7.0°	1.8°	15.1°	9.0°	2.2°

ant. #9 rel. to #1	5.1 MHz			11.5 MHz			18.0 MHz		
elevation	ε_{iso}	ε_{mod}	ε_{meas}	ε_{iso}	ε_{mod}	ε_{meas}	ε_{iso}	ε_{mod}	ε_{meas}
4.5°	5.3°	11.8°	1.6°	12.7°	10.3°	2.9°	12.3°	9.9°	2.9°
11°	5.1°	11.0°	1.6°	11.2°	8.8°	2.9°	12.6°	9.2°	2.9°
19°	5.5°	10.4°	1.6°	10.5°	8.0°	2.9°	10.8°	8.2°	2.9°

ant. #11 rel. to #1	5.1 MHz			11.5 MHz			18.0 MHz		
elevation	ε_{iso}	ε_{mod}	ε_{meas}	ε_{iso}	ε_{mod}	ε_{meas}	ε_{iso}	ε_{mod}	ε_{meas}
4.5°	5.5°	12.4°	1.6°	7.3°	6.6°	4.0°	11.1°	8.4°	3.8°
11°	4.4°	11.0°	1.6°	7.7°	6.2°	4.0°	11.7°	9.1°	3.8°
19°	4.3°	10.2°	1.6°	8.2°	5.2°	4.0°	12.0°	10.6°	3.8°

From these tables, several features can be seen:

1. While it may be expected that the antenna pattern errors are reduced when more information is used in deriving them, this is not always the case. At the lowest frequency (5.1 MHz), the

simple assumptions, of azimuth-independent gain and a phase response based on a spherical wavefront, yield gain and relative phase errors that are less than those obtained with numerical modelling. Likewise, for antenna #11 at the two higher frequencies, the rms errors in gain found with the simple assumptions are less than those found with numerical modelling; this antenna is well-removed from other antennas, and can be expected be influenced more by ground inhomogeneities (not considered in the modelling) than by other conducting elements. It should be noted that in all these cases, the rms errors found using the assumptions tend to be smaller than in other cases, an exception being the relatively large rms gain errors at 5.1 MHz and 4.5° elevation where a distant ground feature [1] influenced the azimuthal antenna patterns.

2. For the remaining frequencies (11.5 and 18.0 MHz) and antennas #5 and #9 (which are near other conducting elements), numerical modelling produced smaller rms pattern errors than those found assuming azimuth independent-gains and spherical-wavefront phase response, as expected.

3. Considering the rms gain and relative-phase errors found in the measurements, it is clear that actual pattern measurements yielded substantially more accurate antenna patterns than the other two approaches, in all cases.

It is worth summarizing Tables 2 and 3 in terms of the rms errors that would result from each of the three techniques, when applied to the present antenna array. Using an azimuth-independent gain assumption yields rms gain errors which range from 0.47 to 1.63 dB, and are greatest for antenna #9 which is near a large conducting element. The spherical-wavefront phase response assumption yields rms relative-phase errors which range from 4.2° at 5.1 MHz to 14.6° at 18.0 MHz. Numerical modelling produces rms gain errors ranging from 0.45 dB to 1.68 dB, the largest errors occurring at 5.1 MHz and 4.5° elevation where a distant ground feature affected the patterns. The rms relative-phase errors with the numerical model lay between 5.2° and 12.6°, with the largest errors occurring at 5.1 MHz. The rms errors resulting from actual measurements are 0.23 to 0.37 dB in gain, and 1.2 to 3.8° in relative phase.

6.0 Conclusions

On the basis of these results, numerical modelling is not expected to be of benefit in determining antenna patterns for HF antenna arrays where conducting elements are sufficiently remote from each other that little interaction occurs, or where significant ground inhomogeneities exist in the vicinity. Modelling is useful, however, when applied to an array of closely-spaced elements, or in considering antennas which are placed near other conducting structures. The precision with which the actual positions and orientations of the conducting elements are modelled is crucial to the success of modelling, as are proper estimates of ground conductivity and antenna feed impedances. Modelling is less likely to be effective at low elevation angles, where the area of ground contributing to the antenna gain is very large, and so likely to include variations in ground parameters which will alter the gain in different directions.

Actual measurement of the antenna patterns yields substantially more accurate antenna patterns than are obtainable through either modelling or simple theory-based assumptions. However, as shown in the previous report [1], measurements must be made at many closely-spaced frequencies in order to permit the resultant element patterns to be reliably interpolated to intermediate frequencies. Good interpolation procedures need to be developed; these procedures might make use of numerical modelling predictions which are fitted to the measured patterns at the measurement frequencies. As ground conditions can change significantly between summer and winter as freezing, thawing and different levels of wetness are experienced, it may be necessary to make measurements and several representative times of year. In any case, measurements should be considered for HF antenna array applications where precise knowledge of the element patterns is required.

References

[1] 'Antenna Amplitude and Phase Pattern Measurements Using an Aircraft-Towed Transmitter', Robert W. Jenkins, CRC Report 95-003, 1995.

[2] 'NEC Modelling of Antenna Array', L.E. Petrie, Contract Report for CRC, Petrie Telecommunications Ltd., 1995.

DOCUMENT CONTROL DATA

(Security classification of title, body of abstract and indexing annotation must be entered when the overall document is classified)

1. ORIGINATOR (the name and address of the organization preparing the document. Organizations for whom the document was prepared, e.g. Establishment sponsoring a contractor's report, or tasking agency, are entered in section 8.)

COMMUNICATIONS RESEARCH CENTRE
3701 CARLING AVENUE, BOX 11490, STATION H
OTTAWA, ONTARIO K2H 8S2

2. SECURITY CLASSIFICATION (overall security classification of the document including special warning terms if applicable)

UNCLASSIFIED

3. TITLE (the complete document title as indicated on the title page. Its classification should be indicated by the appropriate abbreviation (S,C or U) in parentheses after the title.)

A COMPARISON OF MODELLED AND MEASURED HF ANTENNA ARRAY PATTERNS (U)

4. AUTHORS (Last name, first name, middle initial)

JENKINS, ROBERT W. AND PETRIE, LEN E.

5. DATE OF PUBLICATION (month and year of publication of document)

SEPTEMBER 1996

6a. NO. OF PAGES (total containing information. Include Annexes, Appendices, etc.)

24

6b. NO. OF REFS (total cited in document)

2

7. DESCRIPTIVE NOTES (the category of the document, e.g. technical report, technical note or memorandum. If appropriate, enter the type of report, e.g. interim, progress, summary, annual or final. Give the inclusive dates when a specific reporting period is covered.)

CRC TECHNICAL NOTES

8. SPONSORING ACTIVITY (the name of the department project office or laboratory sponsoring the research and development. Include the address.)

DEFENCE RESEARCH ESTABLISHMENT OTTAWA
3701 CARLING AVENUE
OTTAWA, ONTARIO K1A 0K2

9a. PROJECT OR GRANT NO. (if appropriate, the applicable research and development project or grant number under which the document was written. Please specify whether project or grant)

1410-256 AND 1410-250

9b. CONTRACT NO. (if appropriate, the applicable number under which the document was written)

10a. ORIGINATOR'S DOCUMENT NUMBER (the official document number by which the document is identified by the originating activity. This number must be unique to this document.)

CRC-TN-96-002

10b. OTHER DOCUMENT NOS. (Any other numbers which may be assigned this document either by the originator or by the sponsor)

11. DOCUMENT AVAILABILITY (any limitations on further dissemination of the document, other than those imposed by security classification)

(X) Unlimited distribution
( ) Distribution limited to defence departments and defence contractors; further distribution only as approved
( ) Distribution limited to defence departments and Canadian defence contractors; further distribution only as approved
( ) Distribution limited to government departments and agencies; further distribution only as approved
( ) Distribution limited to defence departments; further distribution only as approved
( ) Other (please specify):

12. DOCUMENT ANNOUNCEMENT (any limitation to the bibliographic announcement of this document. This will normally correspond to the Document Availability (11). However, where further distribution (beyond the audience specified in 11) is possible, a wider announcement audience may be selected.)

UNLIMITED

UNCLASSIFIED

SECURITY CLASSIFICATION OF FORM

13. ABSTRACT (a brief and factual summary of the document. It may also appear elsewhere in the body of the document itself. It is highly desirable that the abstract of classified documents be unclassified. Each paragraph of the abstract shall begin with an indication of the security classification of the information in the paragraph (unless the document itself is unclassified) represented as (S), (C), or (U). It is not necessary to include here abstracts in both offical languages unless the text is bilingual).

THE RELATIVE-PHASE RESPONSE AND GAIN PATTERNS FOUND BY NUMERICAL MODELLING OF AN HF ANTENNA ARRAY OF VERTICAL WHIP ANTENNAS ARE COMPARED WITH THE PATTERNS FOUND BY ACTUAL MEASUREMENTS. WHILE SOME FEATURES OF THE MEASURED PATTERNS AGREE WITH THE MODEL, SIGNIFICANT FEATURES DID NOT. THE DISAGREEMENT COULD ORIGINATE FROM GROUND INHOMOGENEITIES AND OTHER LOCAL FEATURES AS WELL AS DIFFERENCES BETWEEN THE ACTUAL AND MODELLED ANTENNA ARRAY SUCH AS DISCREPANCIES IN ANTENNA POSITION AND ORIENTATION, POOR CONNECTIONS TO GROUND RADIALS, AND DIFFERENCES IN THE MODELLED AND ACTUAL ANTENNA LOADING. IN SOME CASES, WHERE THE ELEMENTS WERE CLOSELY SPACED, NUMERICAL MODELLING PROVIDED A SOMEWHAT BETTER ESTIMATE OF THE ANTENNA GAIN AND RELATIVE-PHASE RESPONSE PATTERNS THAN THE SIMPLE ASSUMPTION OF AZIMUTH INDEPENDENT GAINS AND A RELATIVE-PHASE RESPONSE CONSISTENT WITH A SPHERICAL WAVEFRONT CENTERED ON THE TRANSMITTER. HOWEVER, FOR MORE REMOTE ANTENNA ELEMENTS, MODELLING DID NOT PROVIDE A BETTER ESTIMATE; NOR DID IT PROVIDE A BETTER ESTIMATE FOR THE LOWEST MODELLED FREQUENCY. ACTUAL PATTERN MEASUREMENTS, ON THE OTHER HAND PROVIDED SIGNIFICANTLY BETTER PATTERN ESTIMATES IN ALL CASES.

14. KEYWORDS, DESCRIPTORS or IDENTIFIERS (technically meaningful terms or short-phrases that characterize a document and could be helpful in cataloguing the document. They should be selected so that no security classification is required. Identifiers, such as equipment model designation, trade name, military project code name, geographic location may also be included. If possible keywords should be selected from a published thesaurus. e.g. Thesaurus of Engineering and Scientific Terms (TEST) and that thesaurus-identified. If it is not possible to select indexing terms which are Unclassified, the classification of each should be indicated as with the title.)

HF ANTENNA PATTERNS
NEC MODELLING
ANTENNA ARRAYS